https://doi.org/10.5194/egusphere-2025-679
Preprint. Discussion started: 14 March 2025

Reconstruction of reservoir water level-storage relationship based on capacity loss induced by sediment accumulation and its impact on flood control operation

Qiumei Ma[1], Chengyu Xie[1], Zheng Duan[2], Yanke Zhang[1*], Lihua Xiong[3], Chong-Yu Xu[4]

[1] School of Water Resources and Hydropower Engineering, North China Electric Power University, Beijing 102206, China

[2] Department of Physical Geography and Ecosystem Science, Lund University, Sölvegatan 12, 223 62 Lund, Sweden

[3] State Key Laboratory of Water Resources Engineering and Management, Wuhan University, Wuhan 430072, China

[4] Department of Geosciences, University of Oslo, P.O. Box 1047 Blindern, N-0316 Oslo, Norway

Correspondence: Yanke Zhang (zhangyk@ncepu.edu.cn)

Abstract. Sediment accumulation in reservoirs can change the predefined water level-storage (WLS) relationship by significantly reducing the storage capacity, further threatening the flood control safety of reservoirs in long-term scheduling and operation. However, reconstructing the WLS relationship has long been challenging, especially on a large scale, due to the difficulties of traditional field bathymetric measurement. To fill this knowledge gap, a method to estimate the reservoir WLS curve based on the capacity loss induced by sediment accumulation is proposed in this study. To assess the potential negative impact caused by inaccurate WLS curve, flood regulation calculations for reservoirs are performed individually using six design flood hydrographs with return intervals ranging from 200–10,000 years as reservoir inflow. The flood regulation risk is quantified using the maximum flood regulation water level (Z^*) and the ratio of periods exceeding the design flood level (γ). Based on hydrological and sediment data and operational information over ten years, a cascade of nine reservoirs in the Wujiang River in China is selected to conduct the established method.

https://doi.org/10.5194/egusphere-2025-679
Preprint. Discussion started: 14 March 2025

The results show that sediment accumulation is more severe in reservoirs located in the middle and upper reaches of the Wujiang River, leading to the most significant reduction in capacity loss volume for Hongjiadu (180.3 million m³) and the largest loss rate for Suofengying (25.02%) reservoirs. Using the current design WLS curve for flood regulation calculations, Z* is underestimated by 7.11 m and 1.84 m, and γ by 2% and 3% for Suofengying and Dongfeng reservoirs, respectively, compared with the reconstructed one. This underestimation increases with the length of the return interval. This indicates that when storage capacity is considerably reduced, continued use of the existing design WLS curve may significantly underestimate flood regulation risks, thus posing potential safety hazards to the reservoir itself and downstream flood protection objects.

1 Introduction

Reservoirs are artificial or heavily modified water bodies formed using dams, sluices, and other engineering infrastructure for the purpose of regulating river discharge. Reservoirs and dams play a critical role in modern water resources management and utilization by generating electricity, mitigating flood risks, and supplying water (Castelletti et al., 2012; Sen, 2021; Zhou et al., 2021). In the past century, more than 50,000 large reservoirs have been constructed worldwide, regulating over half of the major river systems globally, with a total storage capacity of over 8,000 km³ (Hanasaki et al., 2006). The volume of water stored in these reservoirs exceeds 20% of the world's annual average runoff, equivalent to three times the annual average water storage in all river channels globally, making them crucial elements in the hydrological and biochemical cycles (Yassin et al., 2019). The number of reservoirs under construction and planning continues to increase rapidly to meet the demands of population growth and socioeconomic development, especially in developing countries (Zhong et al., 2020). For instance, China has the largest number of reservoirs in the world, and according to the First Bulletin of the National Water Resources Census, as of 2011, China has a total of 98,002 reservoirs in operation or under construction, with a total

https://doi.org/10.5194/egusphere-2025-679
Preprint. Discussion started: 14 March 2025

storage capacity exceeding 932.3 billion m^3.

Reservoir water storage is a key variable in reservoir hydrology and serves as fundamental information for reservoir scheduling and operational management (Gao, 2015; Liu et al., 2022). The primary method for obtaining reservoir water storage during routine operations is by referring to the water level-storage (WLS) curve, which quantifies the functional relationship between water level and storage based on gauge water level observations. Therefore, the accuracy and reliability of the WLS curve are crucial for determining the characteristic storage capacities of reservoirs, such as the normal storage capacity and flood control storage capacity, which directly influence the effectiveness of subsequent reservoir operations and management decisions. However, the water storage capacity of a reservoir can change during long-term operation due to multiple factors, both natural and anthropogenic, including river diversion, sand mining, and especially sediment deposition. Sediment carried by upstream inflows can be trapped by the dam and thus accumulate in the reservoir, continuously reducing its effective storage capacity. If the extent of sediment accumulation and the storage capacity are not investigated in a timely manner, the outdated design WLS curve will continue to be used, potentially leading to a decline in the functionality and overall benefits of the reservoir, or even causing safety incidents.

There are two main methods that have traditionally been used to reconstruct WLS functional relationship in previous studies. The first method involves conducting topographic surveys in the reservoir area to estimate the reservoir storage capacity. For example, Sawunyama (2006) conducted field measurements of water depth and coordinates in the reservoir to establish a power function between surface area and storage capacity. Zhang et al. (2011) used an in situ bathymetric survey approach to measure the water depth of a high-altitude lake and create isobathic maps to calculate the storage capacity. However, the field measurement method is often limited by long survey durations, complex topography conditions, and high costs, which collectively make updating the WLS curve difficult. In recent years, the launch of high-resolution optical and synthetic aperture radar (SAR) satellites has advanced satellite remote sensing technology, positioning it as a cutting-edge tool in hydrology. These

https://doi.org/10.5194/egusphere-2025-679
Preprint. Discussion started: 14 March 2025

technologies have gradually been applied to reservoirs and dams monitoring, although this is still in its preliminary stages and accuracy needs to be improved (Gourgouletis et al., 2022). By extracting reservoir areas from remote sensing images and combining them with satellite radar altimetry, relationships among reservoir water levels, areas, and storage volumes can be established to reconstruct Z-A-V (Elevation-Area-Volume) curves (Gao et al., 2012; Guan et al., 2021; Li et al., 2020; Zhang et al., 2017).

The second method is based on measured hydrological data to estimate and revise the WLS curve using the water balance principle. Specifically, the WLS curve can be derived from the relationship between water level increments and storage capacity increments detected from hydrological data measured during the dry season (Su Yepeng, 1999). Liu Dezong (1992) transformed the WLS curve calibration problem into an outflow measurement problem through water balance analysis and verified the validity of the reconstructed WLS curve for the Xueye Reservoir. On the other hand, the accuracy of the WLS curve reconstructed using water balance relations is influenced to some extent by the selected data to some extent, and there are challenges in determining certain parameters in the water balance equation. Given the limitations of the above approaches, although numerous previous studies have emphasized the urgent need to recheck the reservoir WLS curve, most reservoirs have not yet conducted storage capacity estimations.

Notably, sediment accumulation in reservoirs offers barriers to natural sediment transport along river courses. Thus it is the key factor leading to the reduction of storage capacity and results in serious problems in operation management (Sedláček et al., 2022). As a result, the loss of reservoir storage capacity in China is the most serious in the world, with an average capacity loss rate of over 11.27%, which is 2 to 4 times the global average (Ran et al., 2013; Zhang et al., 2023). Estimating the storage capacity loss induced by sediment accumulation and reconstructing the WLS curve provides a new direction for the second category of methods (Huang et al., 2018). However, few studies have investigated the validity of reconstructing the WLS curve based on sediment accumulation, and there has been insufficient attention to the practical effectiveness of the reconstructed curve. In particular, the differences in flood

https://doi.org/10.5194/egusphere-2025-679
Preprint. Discussion started: 14 March 2025

regulation performance between the two curves, before and after reconstruction, have not yet been elucidated.

To fill this knowledge gap, this study aims to estimate the WLS relationship of reservoirs by proposing a storage capacity loss rate (LR) indicator based on sediment accumulation and, furthermore, to identify the impact of the reservoir WSL relationship on flood control operations through flood regulation risk indictors. A cascade of nine reservoirs in the Wujiang River is used as a case study to conduct the reservoir WLS curve estimation and impact analysis. Specifically, we seek to address the following scientific questions: (a) What are the characteristics of sediment accumulation among different reservoirs in the selected cascade? (b) Can the reservoir WLS curve be effectively reconstructed using the proposed water storage capacity LR framework, based on long-term water and sediment data? and (c) What is the impact of the outdated design WLS curve on flood control operations?

The remainder of this paper is organized as follows: Section 2 describes the cascade reservoirs located in the Wujiang River basin, along with observed water and sediment data; Section 3 introduces the estimation of the LR indictor, reconstruction of the WLS curve, and detection of flood prevention operation responses on the WLS curves before and after reconstruction; Section 4 presents and discusses the results of our analysis; finally, Section 5 provides the primary conclusions of this study.

2 Study area and data

2.1 study area

The Wujiang River, the largest tributary on the southern bank of the upper reaches of the Yangtze River, is characterized by its considerable natural elevation drop and abundant hydropower resources. The Wujiang River Basin covers a catchment area of 87,920 km² and extends over a length of 1,037 km with a natural fall of 2,124 m, and has a subtropical wet monsoon climate. The basin's integral role in the "West-East Electricity Transmission" project enhances its prominence, establishing it as the critical one of China's thirteen major hydropower bases. The cascade reservoir system of the

https://doi.org/10.5194/egusphere-2025-679
Preprint. Discussion started: 14 March 2025

Wujiang River used in this study comprises nine reservoirs with varying shapes, surface areas, and regulation capacities. The Wujiang River exhibits relatively stable annual runoff. The Hongjiadu (WJD) reservoir, in the upstream section, acts as the "leading reservoir" of the cascade reservoir system, offering multi-year regulation capability. The midstream Wujiangdu (WJD) reservoir provides annual regulation, while the downstream Goupitan (GPT) reservoir also supports multi-year regulation. The spatial distribution of reservoirs in the Wujiang River basin is illustrated in Fig. 1 After the gradual completion of the cascade system in the basin, the Wujiang River Basin has aggravated the interception of sediment. As a result, during long-term operation, the storage capacity of the nine-reservoir cascade system has suffered varying degrees of loss, which has had a potential negative impact on the operation and scheduling of the reservoirs.

Before 1990, the mean sediment accumulation in the capacity of reservoirs along the Wujiang River is about 9 million tons annually, predominantly influenced by large reservoirs, while small and medium-sized reservoirs contribute a minor fraction of the total capacity. From 1991 to 2005, the primary reservoirs that intercepted sediment on the Wujiang River mainstream transitioned to the HJD and DF reservoirs, which were impounded in 1994 and 2004 years, respectively. The average multi-year sediment accumulation in the capacity of reservoirs on the Wujiang River was 16 million tons, reflecting an increase compared with the period from 1956 to 1990, along with a rise in the proportion of sediment accumulation in major reservoirs. Since 2006, although the reservoirs located on the lower reaches of the Wujiang River have gradually completed and began to operate, the HJD and DF Reservoirs in the upper reaches remain the primary reservoirs for sand retention.

https://doi.org/10.5194/egusphere-2025-679
Preprint. Discussion started: 14 March 2025

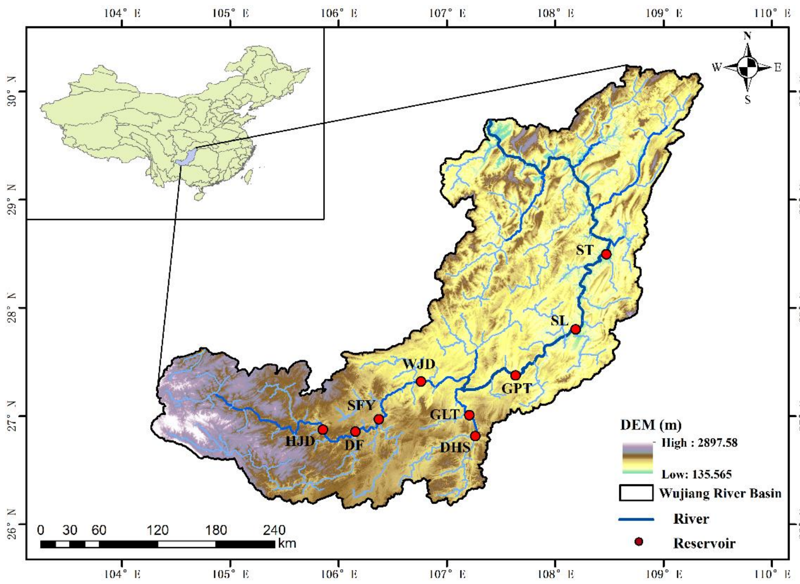

Figure 1. Location of the Wujiang River Basin and cascade reservoirs (HJD, DF, SFY, WJD, GPT, SL, ST, GLT, DHS denote the Hongjiadu and Dongfeng, Suofengying, Wujiangdu, Goupitan, Silin, Shatuo, Goupitan, Geliqiao and Dahuashui Reservoirs, respectively. Same as below.)

2.2 Data

This study collects fundamental hydrological and sediment data, such as sand content in the inflow water, inflow and outflow, and reservoir operation information including total storage capacity, design flood level, and calibration flood level for the nine-reservoir cascade system. Rigorous quality control on the water and sediment data was conducted by manually verifying and rectifying anomalous and erroneous data. The main parameters of each reservoir are presented in Table 1 It is worth noting that the duration of the selected hydrological and sediment data varies from 10 to 23 years during 2001 to 2023 among different reservoirs, due to different beginning time of construction and operation for different reservoirs.

https://doi.org/10.5194/egusphere-2025-679
Preprint. Discussion started: 14 March 2025

Table 1. Basic reservoir information of the Wujiang River

Reservoir	Total storage capacity (10^8 m^3)	Dead storage capacity (10^8 m^3)	Regulating capacity (10^8 m^3)	Normal storage level (m)	Dead water level (m)	Design Flood Level (m)	Calibration Flood Level (m)
HJD	49.47	11.36	33.61	1140	1076.0	1141.34	1145.40
DF	10.25	3.74	4.91	970	936.0	975.69	977.53
SFY	2.01	1.01	0.67	837	822.0	837.97	842.37
WJD	23.0	7.8	13.60	760	720.0	760.30	762.80
GPT	64.54	26.62	29.02	630	590.0	632.89	638.36
SL	15.93	8.88	3.17	440	431.0	445.15	449.45
ST	9.21	4.83	2.87	365	353.5	366.73	369.65
DHS	2.77	1.15	1.355	868	845.0	868.43	871.35
GLQ	0.77	0.51	0.19	719	709.0	719.40	722.58

3 Methods

This study proposes a storage capacity LR indicator based on sediment accumulation to estimate the WLS relationship of reservoirs first. Second, flood regulation calculations are performed at reservoirs with relatively higher LR values, using six design flood hydrographs with different return intervals as typical inflow discharge, to identify the impact of reservoir WSL relationship on flood control operation. Finally, the flood regulation risks are assessed to quantify the response of the scheduling process to the reconstructed WLS relationship. The detailed methods and steps of this study are as follows (Fig. 2).

https://doi.org/10.5194/egusphere-2025-679
Preprint. Discussion started: 14 March 2025

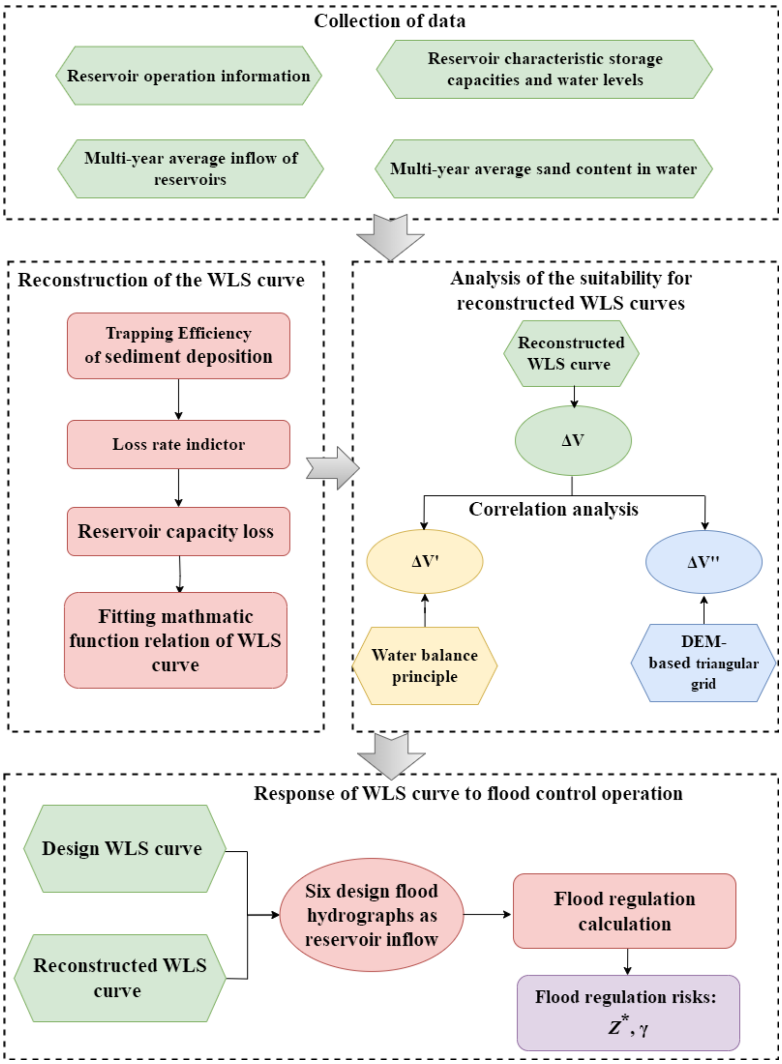

Figure 2. Schematic of the framework in this study.

3.1 Deriving reservoir capacity loss volume and rate due to sediment accumulation

In this study, the reservoir storage capacity LR due to sediment accumulation for each reservoir in the cascade system is calculated based on the inflow series, sand content in inflow water, and total reservoir capacity during the period covered by the documented data. Subsequently, the corrected LR for each reservoir's storage capacity since its construction is determined. For convenience, we assumes that the sediment accumulation is spatio-temporally uniform. That is, the sediment is uniformly

https://doi.org/10.5194/egusphere-2025-679
Preprint. Discussion started: 14 March 2025

distributed in the bottom and the deposition velocity is the same every year. Therefore, the LR represents the proportion of multi-year average reservoir storage capacity loss. The calculation equation of LR is as follows:

$$LR_i = \frac{n_i \times w_i \times Te_i}{\rho \times RC_i} \tag{1}$$

where n_i is the temporal interval of recorded data for the ith reservoir, in the unit of year; RC_i represents the reservoir capacity, measured in 10^8 m³; w_i denotes the long-term average sediment contained in the inflow water of the ith reservoir, quantified in 10^8 kg/a; ρ indicates the density of deposited sediment, expressed in kg/m³; and Te_i reflects the sediment trapping efficiency, initially introduced by Brune (1953) and further extended and popularized by Mulu and Dwarakish et al. (2015) and Liu et al. (2022). The deposition rate of the sediment input into the reservoir represented by Te_i was simplified into the ratio of reservoir capacity to incoming flow, as follows:

$$Te_i = 1 - \frac{0.05\alpha}{\sqrt{\Lambda\tau}} \tag{2}$$

where α is the correction factor; $\Lambda\tau$ is the reservoir stagnation time, $\Lambda\tau = RC_i / Q_i$; and Q_i is the multi-year average inflow water volume at the dam site of the ith reservoir, 10^8 m³.

3.2 Nonlinear fitting of the reservoir WLS relationship

The feature of reservoir capacity can be represented by a series of discrete water level and storage data. However, this can lead to inefficiencies in the algorithmic resolution of the scheduling model. In contrast, quantitative description can enhance the efficiency of various algorithms for solving the scheduling model. Therefore, it is essential to fit the discrete data points of water levels and storages into a functional relationship. In conjunction with the current literature on the fitting of reservoir WLS curves, elementary functions are amalgamated through rational operations to formulate three types of mathematic function (Eqs. 3- 5).

$$Z = f_1(V) = \alpha_1 V^3 + \alpha_2 V^2 + \alpha_3 V + \alpha_4 \tag{3}$$
$$Z = f_2(V) = \beta_1 V^{\beta_2} + \beta_3 \tag{4}$$
$$Z = f_3(V) = \gamma_1 e^{\gamma_2 V} + \gamma_3 e^{\gamma_4 V} \tag{5}$$

where V is the reservoir storage capacity, 10^8 m^3; Z is the concurrent water level, m;

https://doi.org/10.5194/egusphere-2025-679
Preprint. Discussion started: 14 March 2025

and f_1, f_2 and f_3 represent polynomial, power, and exponential functions, respectively.

To assess the goodness-of-fit of the nonlinear models f_1, f_2, and f_3 compared with the discrete data points of reservoir water levels and storages, in this study, we employ three typical statistical indices, including determination coefficient (R^2), sum squared error (SSE), and root mean square error (RMSE) (Eqs. 6- 8).

$$\text{RMSE}=\sqrt{\frac{1}{N}\sum_{i=1}^{N}\left(Z_i-\hat{Z}_i\right)^2} \tag{6}$$

$$R^2=1-\frac{\sum_{i=1}^{N}\left(Z_i-\hat{Z}_i\right)^2}{\sum_{i=1}^{N}\left(Z_i-\bar{Z}_i\right)^2} \tag{7}$$

$$\text{SSE}=\sum_{i=1}^{N}\left(Z_i-\hat{Z}_i\right)^2 \tag{8}$$

where Z_i is the observed water level corresponding to the assessed reservoir capacity V_i, m; $\hat{z}_i$ is the estimated reservoir level, derived from back extrapolation of the reservoir WLS curve, referred to as $\hat{z}_i=f(V_i)$, m; $\bar{Z}_i$ is the average water level, m; and N is the number of discrete data points sampled from reservoir WLS curve used to evaluate the performance of the fitted relationship.

3.3 Reconstructing reservoir WLS curve based on the loss rate

The cumulative storage capacity loss over the period covered by the documented data can be estimated first, based on the corrected storage capacity LR for each reservoir determined in Section 3.1. Second, the total capacity loss is deducted from the original capacity of discrete data points to derive the calibrated water level-storage discrete data points. Third, the optimal line of f_i (i = 1, 2, 3) is fitted to model the calibrated discrete data points of water levels and storages for the nine reservoirs, using the goodness-of-fit evaluation metrics introduced in Section 3.2 and deriving the reconstructed WLS curve, $z=f^{'}(V)$.

In this study, we employ two approaches, i.e., water balance equation and DEM, to indirectly analyze the suitability of the reconstructed WLS curve. For the former, the change of reservoir water storage detected from water balance budgets was compared with that from storage capacity loss. The water storage volume change of the reservoir

https://doi.org/10.5194/egusphere-2025-679
Preprint. Discussion started: 14 March 2025

over any time period is determined by the inflow water volume, outflow water volume, rainfall, evaporation, and seepage using the water balance equation represented in Eq. (9). The summer flood season in the Wujiang River basin is marked by rain storm which results in significant fluctuations in reservoir water storage. During this period, inflow and outflow dominate the variations in reservoir water storage, while the effects of rainfall, evaporation, and seepage on the closure of water balance are comparatively minimal. Consequently, we explore the measured inflow and outflow from April to August 2023 to estimate the change in reservoir water storage $\Lambda V^{'}$ according to water balance relation.

$$\Lambda V^{'} = V_{\text{in}} - V_{\text{out}} - V_{\text{ET}} - V_{\text{seep}} + V_{\text{rain}} \tag{9}$$

where $\Lambda V^{'}$ is the change in reservoir water storage, m³; V_{in} is the volume of inflow water entering the reservoir, m³; V_{out} is the volume of outflow water released from the reservoir, m³; V_{ET} is the volume of water evaporated from the reservoir, m³; V_{seep} is the volume of reservoir leakage water, m³; and V_{rain} is the rainfall water falling into the reservoir surface.

As for the latter approach, we derive some discrete data of water levels and storages based on traditional method with DEM data to quantify the similarity with reconstructed WLS curve. This process primarily involves selecting the Copernicus DEM digital elevation model with a resolution of 30 m to create a digital triangular grid, using the ArcGIS platform to extract the surface area corresponding to each elevation at 1 m intervals, resulting in a series of scatter points representing the relationship between water levels and surface areas, then employing the prismatic table method (Eqs. 10-11) to calculate the reservoir storage capacity changes between adjacent water levels, finally, integrating the volume computed by ArcGIS at the initial elevation surface to derive the WLS curve, which is then compared with the reconstructed and design reservoir WLS curves.

$$V_i = \frac{1}{3}\Delta h\left(S_{i-1} + \sqrt{S_{i-1}S_i} + S_i\right) \tag{10}$$

$$V = \sum_{i=1}^{L} V_i + V_0 \tag{11}$$

where V_i is the difference in reservoir capacity between two neighboring water levels,

10^8 m^3; Δh is the water level difference between two neighboring water levels, m; S_i, $S_{i\text{-}1}$ are the water surface areas corresponding to the two neighboring water levels, m^2; i is the serial number; L is the cumulative number, and V_0 is the initial reservoir capacity, 10^8 m^3.

3.4 Quantifying the response of flood control operation to the WLS curve

To demonstrate the necessity of rechecking current reservoir WLS curve, we select reservoirs with higher LR values to implement the flood regulation calculation to assess the resulting flood risks with reservoir WLS curve before and after the reconstruction, respectively. Six design flood hydrographs with return intervals varying from 200 to 10000 years are individually taken as reservoir inflow discharge to quantify flood operation risks. The flood operation risks are quantified based on the maximum regulation water level (Z^*) and the ratio of the number of time periods in which the characteristic water level is surpassed to the total number of time periods (γ). Flood regulation calculations are conducted utilizing the water balance equation (Eq. 12). If the values of Z^* and γ generated from reconstructed WLS curve exceed those generated using the design WLS curve currently in use, it indicates that continued use of the existing design WLS curve will lead to a potential underestimation of risk in flood control and dispatching.

$$V_2 - V_1 = \frac{(Q_1 + Q_2)}{2} \times \Delta t - \frac{(q_1 + q_2)}{2} \times \Delta t \tag{12}$$

where V_1 and V_2 denote the reservoir storage capacity at the beginning and end of the time period, respectively, m^3; Q_1 and Q_2 are the inflow discharge at the beginning and end of the time period, respectively, m^3/s; q_1 and q_2 are the outflow discharge at the beginning and end of the time period, respectively, m^3/s; and Δt is the length of the time period, h.

4 Results

4.1 Analysis of total reservoir storage capacity loss rate and volume

Figure. 3 illustrates the temporal dynamics of annual average inflow for each reservoir.

https://doi.org/10.5194/egusphere-2025-679
Preprint. Discussion started: 14 March 2025

From Fig. 3, it can be clearly observed that the average annual inflow of reservoirs located at the main stream increases progressively from upstream to downstream of the Wujiang River. Hongjiadu Reservoir acts as the primary reservoir in the cascade system, and shows low annual average inflow of between about 100 to 200 m³/s. Dongfeng, Suofengying, and Wujiangdu Reservoirs exhibit median annual average inflows from 200 to 500 m³/s. In contrast, Goupitan, Silin, and Shatuo Reservoirs receive high annual average inflow between 500 and 1000 m³/s. Dahuashui and Geliqiao Reservoirs are located in the tributaries of the Wujiang River. Thus, their annual average inflow is significantly lower than that of the main stream reservoirs, with a peak annual average inflow of 113.53 m³/s recorded in 2020.

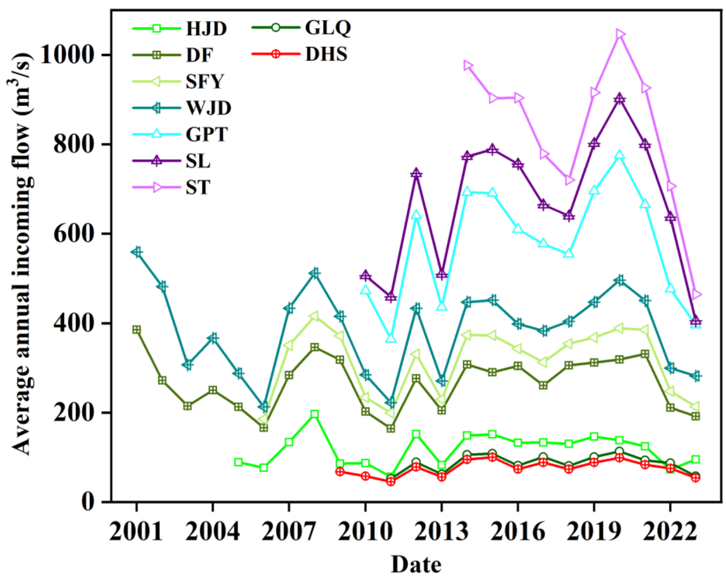

Figure 3. Dynamics of annual average inflow of the cascade reservoirs (The periods covered by inflow data varies due to the reservoirs constructed in tributary and downstream is later than those upstream.)

The intermediate results for deriving the LR of water storage capacity for each reservoir in the cascade system are presented in Table 2 Subsequently, the total reservoir capacity loss attributed to sediment deposition in each reservoir is derived from the reservoir capacity LR, as illustrated in Fig. 4. In Fig. 4, the SFY Reservoir shows the highest value of LR of 25.02%, followed by the DF and WJD Reservoirs with LR of

https://doi.org/10.5194/egusphere-2025-679
Preprint. Discussion started: 14 March 2025

12.96% and 7.84%, respectively. The remaining six reservoirs demonstrate lower capacity loss rates ranging from 0.32% to 4.49%. The WJD Reservoir exhibits the highest volume of capacity loss of 180.3 million m³, followed by the DF, HJD, and SFY Reservoirs with losses of 132.9 million m³, 169.5 million m³, and 50.3 million m³, respectively. The other five reservoirs demonstrate lower capacity losses ranging from 0.035 million m³ to 26.9 million m³. It is indicated that the reservoirs with large capacity losses (exceeding 5%) are situated in the middle and upper reaches of the Wujiang River, in accordance with the principle that upstream reservoirs prioritize the capture of sand in inflow water.

Table 2. Calculation table for the rate of loss of storage capacity

Reservoir	Time interval of data (year)	Sand content of inflow water (kg/m^3)	RC_i (10^8 m^3)	Te_i (%)	w_i (10^8 kg)
HJD	19	1.460	49.470	0.957	53.509
DF	23	1.130	10.250	0.856	94.434
SFY	18	0.609	2.012	0.648	60.428
WJD	23	0.982	23.000	0.885	118.881
GPT	14	0.127	64.540	0.916	22.471
SL	14	0.154	15.930	0.818	31.370
ST	10	0.204	9.210	0.733	51.374
DHS	15	0.228	2.765	0.852	5.390
GLQ	13	0.229	0.774	0.701	5.341

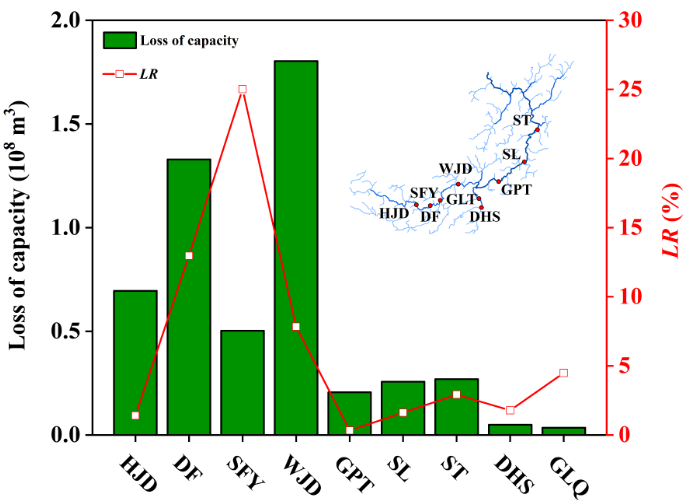

Figure 4. Rate and volume of the storage capacity loss in various reservoirs due to sedimentation accumulation

https://doi.org/10.5194/egusphere-2025-679
Preprint. Discussion started: 14 March 2025

4.2 Reconstructing the reservoir WLS curve

Three mathematic function types, i.e., f_1, f_2, and f_3, were employed to fit the discrete raw water level-storage data points for each reservoir in the Wujiang cascade system, and the statistic indices were quantified to evaluate the goodness-of-fit of the regression coefficients. Figure 5 illustrates that the function type of f_2, with the formula of $Z = f_2(V) = \beta_1 V^{\beta_2} + \beta_3$, demonstrates superior performance in modeling the relationship between reservoir water level and storage across the nine reservoirs. The goodness-of-fit indexes for type f_2 are consistently similar among different reservoirs, reflecting superior fitting performances of f_2 and indicating its applicability and reliability in depicting WLS curve. Conversely, function types of f_1 and f_3 exhibit satisfactory fitting performance in Dongfeng and Wujiangdu Reservoirs; however, they perform poorly in other reservoirs, revealing significant discrepancies among different reservoirs. This suggests that function types of f_1 and f_3 do not fulfill the reliability requirements for all reservoirs, indicating insufficient applicability. Consequently, $Z = f_2(V) = \beta_1 V^{\beta_2} + \beta_3$ is selected as the appropriate fitting function curve for the cascade reservoir system. The original water level-storage discrete point data for each reservoir within this cascade system were fitted to determine the regression coefficients. Subsequently, these parameters were combined with the adopted discrete point data generated by subtracting storage capacity losses, to obtain the new parameters for the reconstructed capacity curves of each reservoir. The regression coefficients in f_2, which are optimized by the Least Squares method, are presented in Table 3.

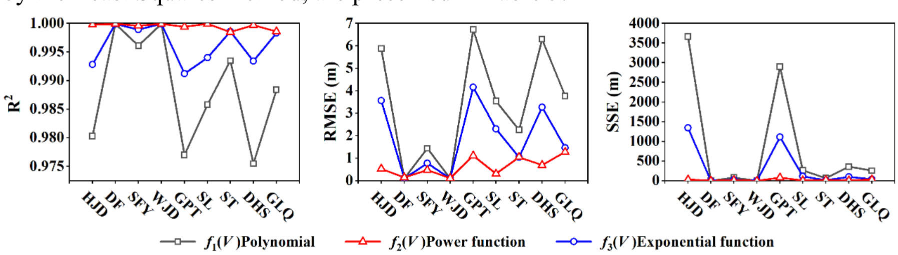

Figure. 5 Goodness-of-fit metrics for the three function types of f_1, f_2 and f_3 to be determined.

https://doi.org/10.5194/egusphere-2025-679
Preprint. Discussion started: 14 March 2025

Table 3. Power function parameters in the WLS curve before and after the reconstruction

Reservoir	β_1	β_2	β_3	$\beta_1^{'}$	$\beta_2^{'}$	$\beta_3^{'}$
HJD	42.057	0.3597	975.20	30.723	0.4107	994.92
DF	71.840	0.3216	826.14	30.266	0.4925	889.29
SFY	69.479	0.3851	751.93	34.466	0.5727	798.90
WJD	67.158	0.2842	599.49	35.327	0.382	649.81
GPT	76.55	0.2643	408.33	58.417	0.3041	432.20
SL	26.977	0.4184	363.50	19.199	0.4939	374.77
ST	39.405	0.3491	284.12	28.707	0.4123	298.69
DHS	78.548	0.3285	761.95	69.373	0.3553	772.59
GLQ	109.79	0.3594	622.56	89.428	0.4318	643.96

*The parameter $\beta_i\,(i=1,2,3)$ represents the regression coefficients of the WLS functional relationship prior to the reconstruction, while the parameter $\beta_i^{'}\,(i=1,2,3)$ demotes the coefficients of the reconstructed WLS function.

Figure 6 illustrates the reconstructed storage capacity curves against the design capacity curves currently used for three reservoirs with the most significant capacity LRs. Sedimentation in the SFY and DF reservoirs is significant, with dead storage capacities decreasing considerably from 101.2 million m³ and 374.0 million m³ to 50.9 million m³ and 241.1 million m³, respectively. This reduction needs be considered in future reservoir scheduling, especially when scheduling for flood near the dead level, due to the capacity loss. In contrast, the WJD Reservoir also maintains a relatively large capacity, with its dead storage capacity decreased from 780.0 million m³ to 599.7 million m³. The storage error resulted from the biased WLS curve can be disregarded at high water levels, while careful attention is required at low water levels, especially near the dead level, as this error significantly affects normal operation.

https://doi.org/10.5194/egusphere-2025-679
Preprint. Discussion started: 14 March 2025

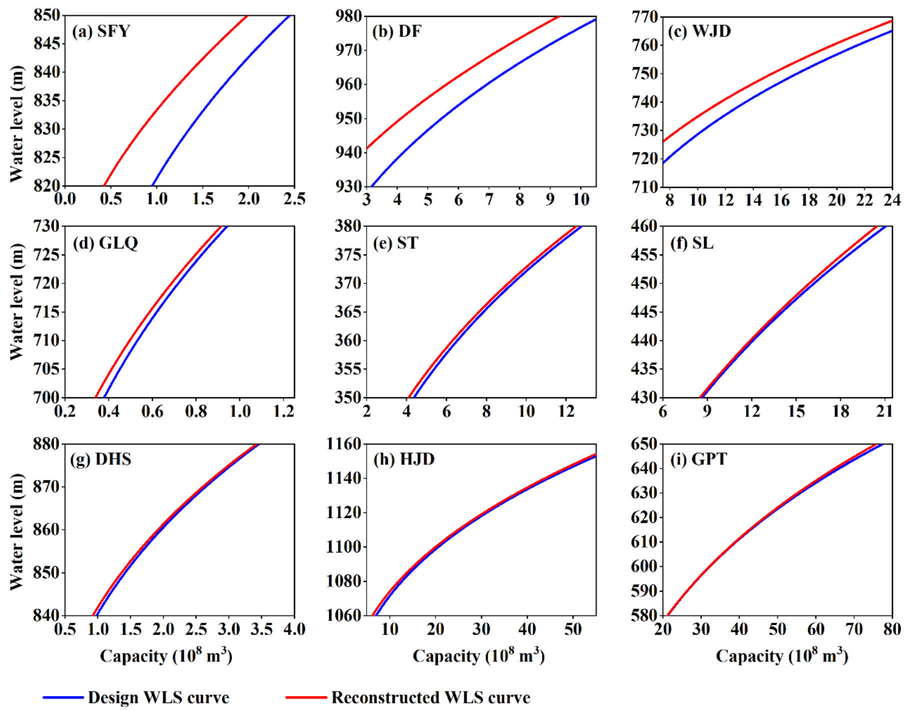

Figure 6. Reservoir capacity curves before and after reconstruction of nine reservoirs

Except these three reservoirs analyzed above, the storage capacity LR of other reservoirs is all below 6%. The capacity curves before and after the reconstruction show median differences. Figure 6 illustrates that the dead capacity of the GLQ and ST reservoirs has decreased from 50.7 million m³ and 483.0 million m³ to 47.2 million m³ and 456.1 million m³, respectively. The error in the reservoir storage capacity curve is negligible during normal operations, but can become significant when the water level approaches the dead water level. In contrast, the SL, DHS, HJD, and GPT reservoirs exhibit minimal sedimentation and lower errors in their capacity curves, ensuring that normal dispatch operations remain unaffected.

4.3 Suitability analysis of the reconstructed reservoir WLS curve

Figure 7 shows the scatter plot of $\Delta V'$, which illustrates the volume change of reservoir water storage derived from the water balance method, against ΔV, which shows the volume change generated from the reconstructed capacity curve based on water level fluctuations. For most reservoirs, the scatters of $\Delta V'$ and ΔV are close to the diagonal

https://doi.org/10.5194/egusphere-2025-679
Preprint. Discussion started: 14 March 2025

1:1 lines and show R^2 values within the range of 0.66-0.98, indicating the general suitability of the reconstructed capacity curve. The scatters of storage changes in the SFY Reservoir exhibit a disorganized distribution of data points, with a R^2 value of only 0.37. This low fitting performance may be attributed to the inflow data of SFY Reservoir, which is primarily caused by abrupt changes in the measured water level at the dam and the irregular fluctuations and negative values of the inflow.

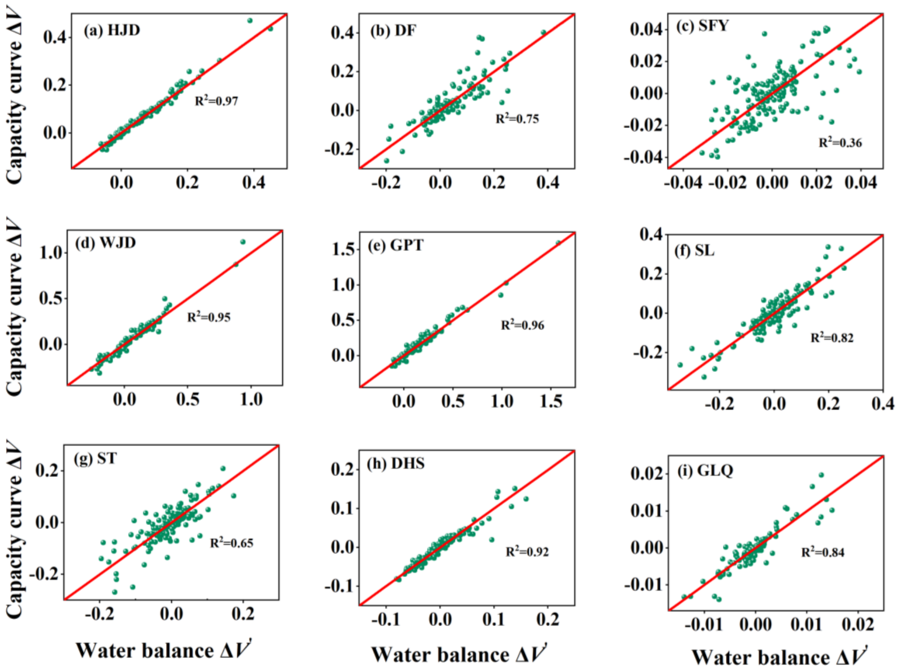

Figure 7. Correlation between the storage changes generated from sediment accumulation and water balance budgets (10^8 m³)

Taking the SFY and DF reservoirs, which show most considerable LR values as example, their DEM data were utilized to compute various scatter data points for water level-capacity. They were then compared with the reconstructed reservoir capacity curves presented in Section 3.2 (Fig. 8). Figure 8 illustrates that the reservoir capacity data points derived from DEM data align more closely with the reconstructed reservoir capacity curves, compared with the existing designs. However, the trends of these curves exhibit slight discrepancies from the reconstructed curves. This suggests that the methodology for assessing reservoir capacity curves proposed in this study more

https://doi.org/10.5194/egusphere-2025-679
Preprint. Discussion started: 14 March 2025

accurately captures the temporal loss of total reservoir capacity. Furthermore, the calculation process is independent of measured data pertaining to reservoir area topography, rendering it both simple and efficient, although it demonstrates some limitations in spatial representativeness. Nonetheless, it lacks spatial representativeness and cannot quantify sediment siltation across the river sections.

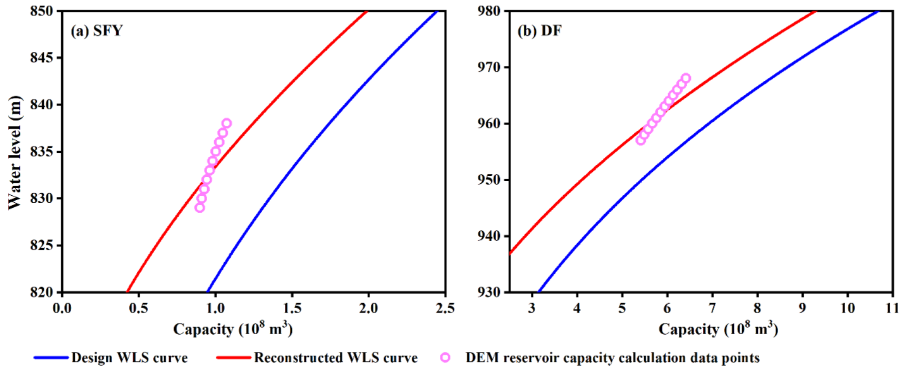

Figure 8. Comparison of reservoir capacity curves reconstructed with DEM and sediment accumulation for Suofengying (SFY) and Dongfeng (DF) reservoirs

4.4 Analysis of the response of flood regulation risk to WLS curve

The flood regulation calculation is focused on the SFY and DF reservoirs, which have the highest and second highest capacity LR. The calibrated flood levels currently used for the SFY and DF reservoirs are 842.37 m and 977.53 m, respectively. The design flood hydrograph was selected for six return intervals ranging from 200 years to 10,000 years with design frequencies of 0.01%, 0.02%, 0.05%, 0.1%, 0.2%, and 0.5% (Fig. 9). The selected design flood hydrograph is conducted with time intervals of 1 hour and durations of 170 hours. Figure 10 presents the operation risk for flood control characterized by Z* and γ individually generated from the design and reconstructed reservoir WLS curves with radar maps. The *Z** values derived from the flood regulation calculation process of reconstructed reservoir WLS curve for both SFY and DF reservoirs exhibit a significant increase with the decreasing design flood frequencies. For the design flood hydrograph with six return intervals, the Z* generated from reconstructed WLS curve is higher than that from the design WLS curve, and the discrepancy between these two Z* increases from 0.20 m to 6.75 m and 0.86 m to 1.84

https://doi.org/10.5194/egusphere-2025-679
Preprint. Discussion started: 14 March 2025

m for the SFY and DF reservoirs, respectively, as the return interval increases from 200 years to 1000 years. In addition, γ is greater than that quantified by the design WLS curve. For the design flood hydrograph with a return interval of 10,000 years, the γ of the SFY Reservoir increased from 22% with the design WLS curve to 23% with the reconstructed WLS curve. Similarly, the proportion of time periods exceeding the normal storage level of the DF Reservoir increased from 18% with design WLS curve to 21% with the reconstructed WLS curve.

The aforementioned results indicate that, according to the prevailing flood control and management principles, both the maximum reservoir water level and the ratio of flood regulation periods surpassing the characteristic water level derived from the existing design capacity WLS curve are lower than those generated from the reconstructed capacity WLS curve. Furthermore, the extent of underestimation escalates with the increasing magnitude of the design flood. If the storage capacity of reservoirs has been significantly reduced, continuing to use the original design capacity WLS curve will lead to an underestimation of the operation risk for flood control. This implies a potential risk of water levels surpassing the designated characteristic level during the actual operational management of the reservoirs, which putting the reservoir and dam infrastructure and downstream flood control at risk. This underscores the imperative for SFY and DF reservoirs to implement the methodology proposed in this study for the timely reconstruction and application of reconstructed capacity curves in future dispatching operations.

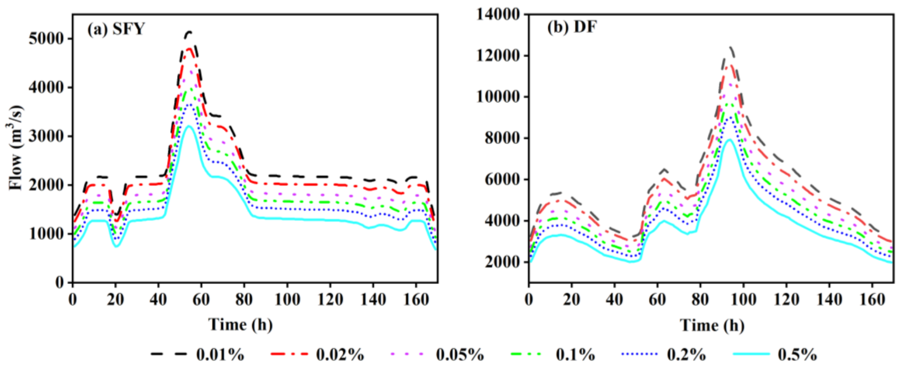

Figure 9. Design flood hydrographs for each frequency at Suofengying (SFY) and Dongfeng (DF) reservoirs

https://doi.org/10.5194/egusphere-2025-679
Preprint. Discussion started: 14 March 2025

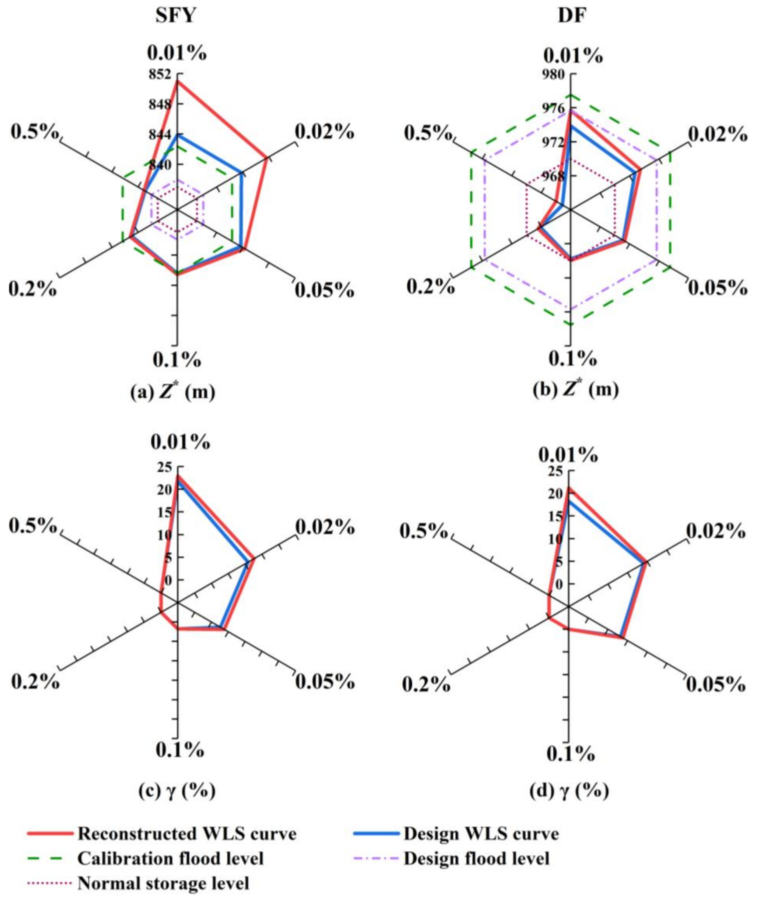

Figure 10. Summary in risk indictors of the flood regulation calculations for Suofengying (SFY) and Dongfeng (DF) reservoirs

5 Discussion

5.1 Reasonableness and uncertainty in reconstructed reservoir WLS curve

Although the WLS curve reconstructed by traditional field measurements with surveying and mapping technology is of high accuracy, the implementation of this method is often limited by the associated challenges in high cost, complex topographic conditions and long duration. Thus the in-situ WLS curve is lacking, and we cannot directly quantify the accuracy of the WLS curve reconstructed in this study. To analyze the reasonableness of the estimated WLS curve, we indirectly compare it with those

https://doi.org/10.5194/egusphere-2025-679
Preprint. Discussion started: 14 March 2025

derived from water balance principle (Ahmad et al., 2022) and high resolution DEM data (Vanthof and Kelly, 2019). The correlation analysis in Section 4.3 indicates that the WLS curve generated from the water balance approach and the DEM approach is much similar to the reconstructed one than the design one for each reservoir.

For estimation of the reservoir storage capacity, there are tradeoffs between accuracy and both spatial scale of reservoirs and the suitable degree of explanatory variables considered. In this study, the storage capacity derived from the WLS relationship and used for a specific reservoir achieves a higher performance of the mathematic model (R2 >0.98), due to the water levels used here directly being correlated with the storages. In contrast, a previous study, which estimates storage capacity for multiple reservoirs on a large scale with 16 influencing factors including reservoir morphological parameters, underlying basin conditions, and climate types, performs significantly worse (with the highest correlation coefficient < 0.97) (Yuan et al., 2024).On the other hand, the XGBoost model driven by 16 explanatory factors is suitable for large scale application, such as, the prediction of reservoir storage capacities on national scale in that study.

In addition, the spatial pattern of storage capacity loss volumes and rates is reasonable among different reservoirs in the cascade. Both larger capacity loss volumes and rates occur for the three or four reservoirs situated at middle and upper reach of the river. This is highly consistent with the conclusion of more serious sediment accumulation in the upper reaches and the priority of the upper reservoir for trapping sands (Brush, 1989). This fundamental pattern indirectly offers another evidence of the reasonableness for the reconstructed WLS curves. In summary, our study contributes a sediment accumulation-based reservoir capacity loss framework to reliably estimate WSL relationships for multiple reservoir on a larger scale.

5.2 Limitations of the proposed framework and further efforts

Apart from sediment accumulation, other factors, such as river diversion and sand mining, can result in the change of reservoir storage capacity. In this study, we consider sediment accumulation as the most important one to influence the storage capacity,

https://doi.org/10.5194/egusphere-2025-679
Preprint. Discussion started: 14 March 2025

while ignore other secondary factors. This situation is practical for the selected cascade reservoir system in the Wujiang River. If the framework is to be applied to other reservoirs, the applicability of this assumption should be carefully diagnosed first. Furthermore, there are one potential limitation of the proposed framework, which needs to be improved in further study. Therefore, the framework used to reconstruct WLS relationship is available under relatively strict constraints. Specifically, we assume the temporal velocity and spatial distribution of sediment accumulation are uniform using the ratio of reservoir storage capacity to incoming flow (Te_i) defined in the mathematic relationship of Eq. (2), to simplify the calculation of storage capacity loss rate. In fact, dams and reservoirs are complex depositional systems for sediment, which vary with reservoir bottom shapes, total volumes of stored water, river discharges, sediment loads and sediment textures, and universal depositional models (Sedláček et al., 2022). Thus, detailed sedimentation processes in reservoirs are more general and expected in the next attempt. In the future, we will try to introduce physically-based hydrological models coupled with reservoir models (Dong et al., 2022), deep learning algorithms (Cao et al., 2020), and more public available explanatory factors including those extracted from remote sensing missions (Bonnema and Hossain, 2019; Guan et al., 2021) with more flexible non-linear change in sedimentation, to reduce the complexity of reconstructing reservoir WLS relationship, especially on a large scale.

6 Conclusions

As intensified climate change and human activities exert a stronger influence on hydrological process and water balance, improved representation of reservoir WLS curves is valuable for developing more useful flood control adaptation measures. In this study, we contribute a framework to reconstruct reservoir water level-storage (WLS) curve by first constructing a reservoir capacity loss rate (LR) indicator caused by sediment accumulation. Then, flood regulation calculations of reservoirs are performed individually using six design flood hydrographs with six return intervals ranging from 200 to 10,000 years as reservoir inflow, to elucidate the response of reservoir flood

https://doi.org/10.5194/egusphere-2025-679
Preprint. Discussion started: 14 March 2025

control operation to reconstructed WLS curve. Finally, the flood control risk is quantified, using the maximum flood control water level (Z*) and the number of periods exceeding the design flood level (γ). A cascade system of nine reservoirs in the Wujiang River in China is selected to implement the established framework. The main conclusions are as follows:

(1) The results presented in this study demonstrate that the framework of reservoir storage loss volumes and rates induced by sediment accumulation can reconstruct suitable reservoir WLS relationship.

(2) The sediment accumulation in the Suofengying, Dongfeng, and Wujiangdu reservoirs, which are located in the upper reaches of the Wujiang mainstream, is more serious, resulting in significant capacity changes with the LR values over 25.02%, 12.96%, and 10%, respectively. The higher correlation between the water storage changes generated from reconstructed WLS curves in this study and those based on water balance and DEM data demonstrates the suitability of the estimated WLS curve associated with sediment accumulation.

(3) The use of the current design WLS curve for flood regulation calculations underestimates the maximal water level during flood regulation (Z*) and the duration of regulation beyond the characteristic water level (γ). The underestimation increases with the return period of the design flood. For the Suofengying and Dongfeng reservoirs, the underestimation of Z* increases from 0.20 m and 0.86 m for the 200-year return period to 6.75 m and 1.84 m for the 10,000-year return period. This indicates that when the storage capacity is significantly reduced, the continued use of the existing design WLS curve may significantly underestimate the flood regulation risks, thus posing potential safety hazards to reservoir itself and downstream flood protection objects.

Declaration of competing interest

The authors declare that they have no known competing financial interests or personal relationships that could have appeared to influence the work reported in this paper.

Data availability

Data will be made available upon request (qiumeima@ncepu.edu.cn).

Author contributions

YZ, QM and ZD designed the study. QM, CX, ZD, and CYX developed the models, with QM and CX implementing them. CX drafted the manuscript in close collaboration with YZ, QM and CX contributed to the data curation. Throughout the study period, all the authors engaged in discussions regarding the results, provided critical feedback, and approved the final version of the paper.

Acknowledgments

We are very grateful to the reviewers for their input, which significantly improved this paper.

Financial support

This study was funded by the National Natural Science Foundation of China (52109016, U2240201), and the Fundamental Research Funds for the Central Universities (2023MS075, 2024JC003). Additionally, we are very grateful to the editors and anonymous reviewers for their valuable comments, which cloud greatly improve the quality of the paper.

References

Ahmad, M. J., Cho, G., and Choi, K. S.: Historical climate change impacts on the water balance and storage capacity of agricultural reservoirs in small ungauged watersheds, Journal of Hydrology: Regional Studies, 41, 101114, 2022.

Bonnema, M. and Hossain, F.: Assessing the potential of the surface water and ocean topography mission for reservoir monitoring in the mekong river basin, Water Resour. Res., 55, 444-461, 2019.

Brune, G. M.: Trap efficiency of reservoirs, Eos, Transactions American Geophysical Union, 34, 407-418, 1953.

Brush, G. S.: Rates and patterns of estuarine sediment accumulation, Limnol. Oceanogr., 34, 1235-1246, 1989.

Cao, Z., Ma, R., Duan, H., Pahlevan, N., Melack, J., Shen, M., and Xue, K.: A machine learning approach to estimate chlorophyll-a from landsat-8 measurements in inland lakes, Remote Sens. Environ., 248, 111974, 2020.

Castelletti, A., Pianosi, F., Quach, X., and Soncini-Sessa, R.: Assessing water reservoirs management and development in northern vietnam, Hydrol. Earth Syst. Sci., 16, 189-199, 2012.

Dezhong, L.: Preliminary study on calibrating reservoir capacity curves using the water balance method, 1992, 6-9, 1992.

Dong, N., Wei, J., Yang, M., Yan, D., Yang, C., Gao, H., Arnault, J., Laux, P., Zhang, X., and Liu, Y.: Model estimates of china's terrestrial water storage variation due to reservoir operation, Water Resour. Res., 58, e2021WR031787, 2022.

Gao, H.: Satellite remote sensing of large lakes and reservoirs: from elevation and area to storage, Wiley

https://doi.org/10.5194/egusphere-2025-679
Preprint. Discussion started: 14 March 2025

Interdisciplinary Reviews: Water, 2, 147-157, 2015.

Gao, H., Birkett, C., and Lettenmaier, D. P.: Global monitoring of large reservoir storage from satellite remote sensing, Water Resour. Res., 48, W9504, 2012.

Gourgouletis, N., Bariamis, G., Anagnostou, M. N., and Baltas, E.: Estimating reservoir storage variations by combining sentinel-2 and 3 measurements in the yliki reservoir, greece, Remote Sens., 14, 1860, 2022.

Guan, T., Xu, Q., Chen, X., and Cai, J.: A novel remote sensing method to determine reservoir characteristic curves using high-resolution data, Hydrol. Res., 52, 1066-1082, 2021.

Hanasaki, N., Kanae, S., and Oki, T.: A reservoir operation scheme for global river routing models, J. Hydrol., 327, 22-41, 2006.

Huang, K., Ye, L., Chen, L., Wang, Q., Dai, L., Zhou, J., Singh, V. P., Huang, M., and Zhang, J.: Risk analysis of flood control reservoir operation considering multiple uncertainties, J. Hydrol., 565, 672-684, 2018.

Li, Y., Gao, H., Zhao, G., and Tseng, K.: A high-resolution bathymetry dataset for global reservoirs using multi-source satellite imagery and altimetry, Remote Sens. Environ., 244, 111831, 2020.

Liu, C., Hu, R., Wang, Y., Lin, H., Zeng, H., Wu, D., Liu, Z., Dai, Y., Song, X., and Shao, C.: Monitoring water level and volume changes of lakes and reservoirs in the yellow river basin using icesat-2 laser altimetry and google earth engine, J. Hydro-Environ. Res., 44, 53-64, 2022.

Liu, S., Li, D., Liu, D., Zhang, X., and Wang, Z.: Characteristics of sedimentation and sediment trapping efficiency in the three gorges reservoir, china, Catena, 208, 105715, 2022.

Mulu, A. and Dwarakish, G. S.: Different approach for using trap efficiency for estimation of reservoir sedimentation. An overview, Aquatic Procedia, 4, 847-852, 2015.

Ran, L., Lu, X. X., Xin, Z., and Yang, X.: Cumulative sediment trapping by reservoirs in large river basins: a case study of the yellow river basin, Glob. Planet. Change, 100, 308-319, 2013.

Sawunyama, T., Senzanje, A., and Mhizha, A.: Estimation of small reservoir storage capacities in limpopo river basin using geographical information systems (gis) and remotely sensed surface areas: case of mzingwane catchment, Physics and Chemistry of the Earth, Parts a/B/C, 31, 935-943, 2006.

Sedláček, J., Bábek, O., Grygar, T. M., Lenďáková, Z., Pacina, J., Atojdl, J., Hošek, M., and Elznicová, J.: A closer look at sedimentation processes in two dam reservoirs, J. Hydrol., 605, 127397, 2022.

Sen, Z.: Reservoirs for water supply under climate change impact—a review, Water Resour. Manag., 35, 3827-3843, 2021.

Su Yepeng, H. W.: Method for adjusting reservoir capacity curves based on the principle of water balance, Renmin Changjiang (in Chinese), 30, 39-41, 1999.

Vanthof, V. and Kelly, R.: Water storage estimation in ungauged small reservoirs with the tandem-x dem and multi-source satellite observations, Remote Sens. Environ., 235, 111437, 2019.

Yassin, F., Razavi, S., Elshamy, M., Davison, B., Sapriza-Azuri, G., and Wheater, H.: Representation and improved parameterization of reservoir operation in hydrological and land-surface models, Hydrol. Earth Syst. Sci., 23, 3735-3764, 2019.

Yuan, C., Liu, C., Fan, C., Liu, K., Chen, T., Zeng, F., Zhan, P., and Song, C.: Estimation of water storage capacity of chinese reservoirs by statistical and machine learning models, J. Hydrol., 630, 130674, 2024.

Zhang, B., Wu, Y., Zhu, L., Wang, J., Li, J., and Chen, D.: Estimation and trend detection of water storage at nam co lake, central tibetan plateau, J. Hydrol., 405, 161-170, 2011.

Zhang, H., Chen, F., Wang, L., Wang, N., and Yu, B.: Reservoir inventory for china in 2016 and 2021, Sci. Data, 10, 609, 2023.

https://doi.org/10.5194/egusphere-2025-679
Preprint. Discussion started: 14 March 2025

Zhang, L. F., Pan, H. H., Shan, D. J., Zhang, W., and Liang, L.: Remote sensing technology-based rechecking of reservoir storage capacity curve of zhelin reservoi, Water Resources and Hydropower Engineering, 6, p1-p6, 2017.

Zhong, R., Zhao, T., and Chen, X.: Hydrological model calibration for dammed basins using satellite altimetry information, Water Resour. Res., 56, e2020WR027442, 2020.

Zhou, X., Polcher, J., and Dumas, P.: Representing human water management in a land surface model using a supply/demand approach, Water Resour. Res., 57, e2020WR028133, 2021.